

RHIC data and the multichain Monte Carlo DPMJET-III *

F.W.Bopp, J. Ranft^a, R.Engel^b, and S.Roesler^c

^aFachbereich Physik, Universität Siegen,
D-57068 Siegen, Germany

^bForschungszentrum Karlsruhe, Institut für Kernphysik,
Postfach 3640, D-76021 Karlsruhe, Germany

^cCERN, Geneva, Switzerland

Using data from RHIC we are able to systematically improve the two-component Dual Parton Model (DPM) event generator DPMJET-III. Introducing percolation parametrized as fusion of chains the model describes multiplicities and pseudorapidity distributions in nucleus-nucleus collisions at all centralities. Guided by the d-Au data from RHIC we recalibrate the model to obtain collision scaling in h-A and d-A collisions.

1. Introduction

Hadronic collisions at high energies involve the production of particles with low transverse momenta, the so-called *soft* multiparticle production. The theoretical tools available at present are not sufficient to understand this feature from QCD alone and phenomenological models are typically applied in addition to perturbative QCD. The Dual Parton Model (DPM) [1] is such a phenomenological model and its fundamental ideas are presently the basis of many of the Monte Carlo implementations of soft interactions.

One of the most prominent features of the Dual Parton Model has been so far the independent production and decay of hadronic strings. It seems, it is just this feature, which has to be modified in the extremely dense hadronic systems produced in central heavy ion collisions.

2. Two-component Dual Parton Model

2.1. Hadron-hadron collisions, the Monte Carlo Event Generator PHOJET

PHOJET1.12 [2,3] is a modern, DPM and perturbative QCD based event generator describing hadron-hadron interactions and also hadronic interactions involving photons. PHOJET replaces

the original DTUJET model [4], which was the first implementation of this combination of perturbative QCD and the DPM.

The DPM combines predictions of the large N_c, N_f expansion of QCD [5] and assumptions of duality [6] with Gribov's reggeon field theory [7]. PHOJET, being used for the simulation of elementary hadron-hadron, photon-hadron and photon-photon interactions with energies greater than 5 GeV, implements the DPM as a two-component model using Reggeon theory for soft and leading order perturbative QCD for hard interactions. Each PHOJET collision includes multiple hard and multiple soft pomeron exchanges, as well as initial and final state radiation. In PHOJET perturbative QCD interactions are referred to as hard Pomeron exchange. In addition to the model features as described in detail in [8], the version 1.12 incorporates a model for high-mass diffraction dissociation including multiple jet production and recursive insertions of enhanced pomeron graphs (triple-, loop- and double-pomeron graphs).

High-mass diffraction dissociation is simulated as pomeron-hadron or pomeron-pomeron scattering, including multiple soft and hard interactions [9]. To account for the nature of the pomeron being a quasi-particle, the CKMT pomeron structure function [10] with a hard gluonic component is used. These considerations refer to pomeron ex-

*Based on a poster submitted to the 17th International Conference on Ultra Relativistic Nucleus Nucleus Collisions, Jan. 11-17, Oakland, California USA

change reactions with small pomeron-momentum transfer, $|t|$. For large $|t|$ the rapidity gap production (e.g. jet-gap-jet events) is implemented on the basis of the color evaporation model [11].

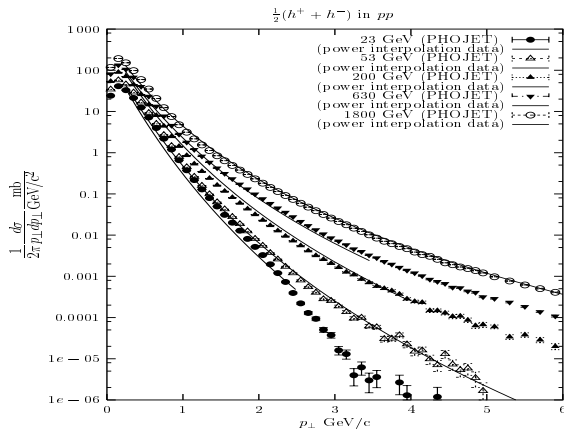


Figure 1. *Transverse momentum distributions of charged hadrons. The results of PHOJET (points) are compared to experimental data represented by lines, fitted to the data points. The data at $\sqrt{s} = 23$ and 53 GeV are from the CERN-ISR[12], the data at 200 GeV are from the UA1 Collaboration[13] and the data at 630 and 1800 GeV are from the CDF Collaboration[14].*

The basic building blocks formed in these processes are color neutral strings. These strings are hadronized in PHOJET using the Lund model as implemented in PYTHIA [15].

PHOJET has been extensively tested against data in hadron-hadron collisions [8]. Furthermore, in a number of papers LEP Collaborations compare many features of hadron production in $\gamma\text{-}\gamma$ collisions to PHOJET, a rather good agreement is usually found.

In Fig.1 we compare charged hadrons according to PHOJET against practically all data on transverse momentum distributions in p-p and \bar{p} -p collisions from colliders. Please note, the points in this Figure are from the PHOJET Monte Carlo, the data are represented by lines, fits to the data points.

2.2. Collisions involving nuclei, the Monte Carlo Event Generator DPMJET-III

The DPMJET-III code system [16,17] is a Monte Carlo event generator implementing Gribov-Glauber theory for collisions involving nuclei, for all elementary collisions it uses the DPM as implemented in PHOJET. DPMJET-III is unique in its wide range of application simulating hadron-hadron, hadron-nucleus, nucleus-nucleus, photon-hadron, photon-photon and photon-nucleus interactions from a few GeV up to cosmic ray energies.

The Gribov-Glauber Multiple Scattering Formalism: Since its first implementations [18,19] DPMJET uses the Monte Carlo realization of the Gribov-Glauber multiple scattering formalism according to the algorithms of [20] and allows the calculation of total, elastic, quasi-elastic and production cross sections for any high-energy nuclear collision. Parameters entering the hadron-nucleon scattering amplitude (total cross section and slope) are calculated within PHOJET.

Realistic nuclear densities and radii are used for light nuclei and Woods-Saxon densities otherwise.

During the simulation of an inelastic collision the above formalism samples the number of “wounded” nucleons, the impact parameter of the collision and the interaction configurations of the wounded nucleons. Individual hadron-nucleon interactions are then described by PHOJET including multiple hard and soft pomeron exchanges, initial and final state radiation as well as diffraction.

As a new feature, DPMJET-III allows the simulation of enhanced graph cuts in non-diffractive inelastic hadron-nucleus and nucleus-nucleus interactions. For example, in an event with two wounded nucleons, the first nucleon might take part in a non-diffractive interaction whereas the second one scatters diffractively producing only very few secondaries. Such graphs are predicted by the Gribov-Glauber theory of nuclear scattering but are usually neglected. Further features of DPMJET-III are a formation zone intranuclear cascade [21] and the implementation of certain baryon stopping diagrams [22].

DPMJET-III and earlier versions like DPMJET-II have been extensively tested against data in hadron-nucleus and nucleus-nucleus collisions [16–18,23]. The code is used for the simulation of cosmic ray showers [24].

3. Comparing the original DPMJET-III with RHIC data

3.1. p–p collisions at 200 GeV

In Fig.2 we compare the preliminary π^0 transverse momentum distribution in p–p collisions at $\sqrt{s} = 200$ GeV from PHENIX [25] to PHOJET and find excellent agreement up to transverse momenta of about $p_{\perp} = 10$ GeV/c.

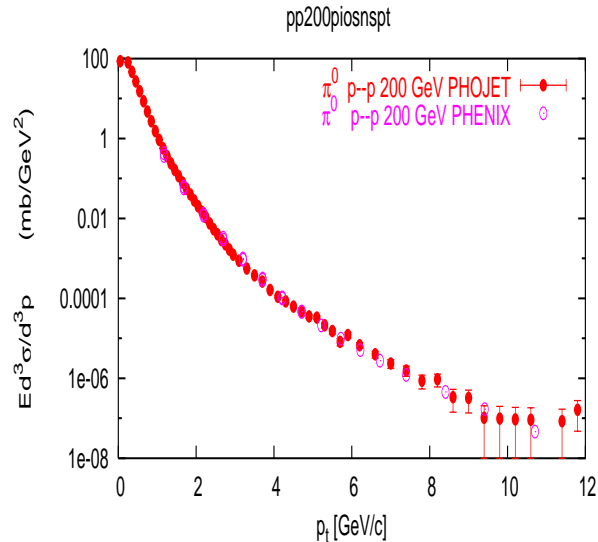


Figure 2. *Transverse momentum distributions of π^0 -mesons produced in $\sqrt{s} = 200$ GeV p–p collisions. The results of PHOJET are compared to preliminary experimental data from the PHENIX-Collaboration [25].*

3.2. Au–Au collisions at 130 GeV in requiring Percolation

The groups at Lisboa [26–28] and Santiago de Compostela [29] were the first to point out, that the multiplicities measured at RHIC are significantly lower than predicted by conventional multi-string models. A new process is needed to lower the multiplicity in situations with a very

high density of produced hadrons like in central nucleus–nucleus collisions. The percolation process, which leads with increasing density to more and more fusion of strings, is one such mechanism [30,31].

Using the original DPMJET-III with enhanced baryon stopping and a centrality of 0 to 5 % we compare to some multiplicities measured in Au–Au collisions at RHIC for $\sqrt{s}_{NN} = 130$ GeV.

	N_{ch}	$dN_{ch}/d\eta _{\eta=0}$
DPMJET-III	6031	968
BRAHMS [32]	3860 ± 300	553 ± 36
PHOBOS [33]		613 ± 24
PHENIX [34]		622 ± 41

This comparison of DPMJET-III with multiplicity data from RHIC confirms: there is a new mechanism needed to reduce N_{ch} and $dN_{ch}/d\eta|_{\eta=0}$ in situations with a produced very dense hadronic system. Therefore, in the next Section we will introduce percolation and chain fusion into DPMJET-III.

4. Percolation of hadronic strings in the modified DPMJET-III

We consider only the percolation with fusion of complete soft chains, these are chains where the transverse momenta of both chain ends is below a certain cut-off p_{\perp}^{fusion} . At the moment we use $p_{\perp}^{fusion} = 2$ GeV/c. The condition of percolation is, that the chains overlap in transverse space. We calculate the transverse distance of the chains L and K R_{L-K} and allow fusion of the chains for $R_{L-K} \leq R^{fusion}$. At the moment we use $R^{fusion} = 0.75$ fm. This procedure is certainly the simplest approximation. A better procedure could be to introduce p_{\perp} dependent transverse dimensions of the chains and then check for percolation.

The chains in DPMJET are fragmented using the Lund code JETSET as available inside the PYTHIA code [15]. Only the fragmentation of color triplet–antitriplet chains is available in JETSET, however fusing two arbitrary chains could result in chains with other colors. Therefore at the moment we select only chains for fusion, which

again result in triplet–antitriplet chains. Examples for the fusion of two chains are:

- (i) A $q_1 - \bar{q}_2$ plus a $q_3 - \bar{q}_4$ chain
become a $q_1 q_3 - \bar{q}_2 \bar{q}_4$ chain.
- (ii) A $q_1 - q_2 q_3$ plus a $q_4 - \bar{q}_2$ chain
become a $q_1 q_4 - q_3$ chain.

Examples for the fusion of three chain are:

- (iii) A $q_3 - q_1 q_2$, a $q_4 - \bar{q}_1$ plus a $\bar{q}_3 - q_5$ chain
become a $q_4 - q_2 q_5$ chain.
- (iv) A $q_4 - \bar{q}_1$, a $q_5 - \bar{q}_3$ plus a $\bar{q}_5 - q_1$ chain
become a $q_4 - \bar{q}_3$ chain.

The expected results of these transformations are a decrease of the number of chains. Even if the fused chains have a higher energy than the original chains, the result will be a decrease of the hadron multiplicity $N_{hadrons}$. In reaction (i) we observe new diquark and anti–diquark chain ends. In the fragmentation of these chains we expect baryon–antibaryon production anywhere in the rapidity region of the collision. Therefore, (i) helps to shift the antibaryon to baryon ratio of the model into the direction as observed in the RHIC experiments.

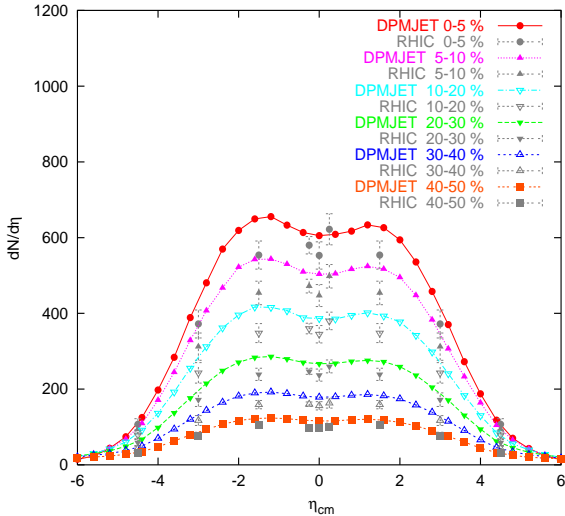


Figure 3. Pseudorapidity distributions of charged hadrons in Au–Au collisions at $\sqrt{s_{NN}} = 130$ GeV for centralities 0–5 % up to 40–50 %. The points (with rather small error bars) are from the DPMJET–III Monte Carlo with chain fusion as described in the text. With two exceptions data points are from the BRAHMS Collaboration [32]. The $\eta=0.0$ points displayed at $\eta=0.25$ are from PHENIX [34] and the $\eta=0.0$ points displayed at $\eta=-0.25$ are from PHOBOS [33].

4.1. d–Au collisions in DPMJET–III

d–Au collisions are the first example where percolation with fusion of chains is found to be important. Pseudorapidity distribution of charged hadrons produced in minimum bias $\sqrt{s} = 200$ GeV d–Au collisions were measured at RHIC by the PHOBOS–Collaboration [35]. In Fig.4 we compare the PHOBOS data to DPMJET–III calculations. Using DPMJET–III without percolation with fusion of chains we find the DPMJET distribution above the experimental data outside the systematic errors. Using DPMJET–III with fusion of chains we find the DPMJET distribution within the systematic errors.

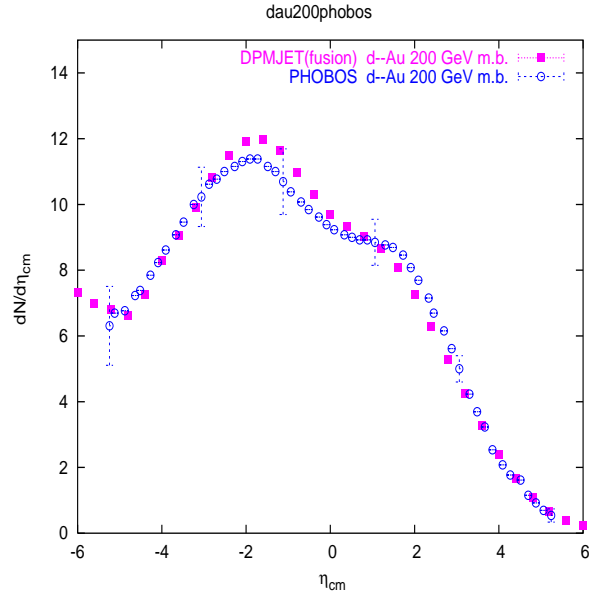


Figure 4. Pseudorapidity distribution of charged hadrons produced in minimum bias $\sqrt{s} = 200$ GeV d–Au collisions. The results of DPMJET with percolation with fusion of chains are compared to experimental data from the PHOBOS–Collaboration [35]. We give at some pseudorapidity values the systematic errors as estimated by the experimental collaboration.

Several RHIC experiments (see for instance [36]) find in d–Au collisions at large p_{\perp} a nearly perfect collision scaling for π^0 production. (Collision scaling means $R_{AA} \approx 1.0$.) The R_{AA} ratios

are defined as follows:

$$R_{AA} = \frac{\frac{d^2}{dp_{\perp}d\eta} N^{A-A}}{N_{binary}^{A-A} \cdot \frac{d^2}{dp_{\perp}d\eta} N^{N-N}} \quad (1)$$

Here N_{binary}^{A-A} is the number of binary Glauber collisions in the nucleus–nucleus collision A–A.

DPMJET–III in its original form gave for π^0 production in d+Au collisions strong deviations from collision scaling ($R_{AA} \approx 0.5$ at large p_{\perp}). The reason for this was in the iteration procedure to sample the multiple collisions in DPMJET: some soft and hard collisions were rejected by this iteration procedure. Using a reordered iteration procedure it was possible to obtain a nearly perfect collision scaling, see Fig. 5.

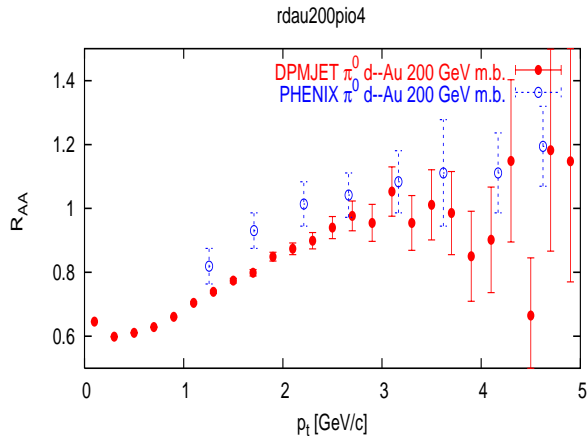


Figure 5. R_{AA} ratio of π^0 -mesons produced in $\sqrt{s} = 200$ GeV d–Au collisions. The results of the modified DPMJET are compared to experimental data from the PHENIX–Collaboration [36].

4.2. Au–Au collisions in DPMJET–III

Our DPMJET–III studies on hadron production in central Au–Au collisions are still in a rather preliminary status. DPMJET–III in its original form gave for π^0 production in central Au+Au collisions strong deviations from collision scaling. In contrast to the low p_{\perp} behavior, the π^0 production at large p_{\perp} was rather similar to the STAR–data[37]. Central to that behavior was that in the iteration procedure to implement the multiple collisions in DPMJET–III some soft and hard collisions were rejected.

The RHIC data on hadron production in d–Au collisions made it clear, that this iteration procedure had to be changed in such a way that no essential deviations from collision scaling occur in d–Au collisions. The same corrections to the iteration procedure then also influence Au–Au collisions in a way, that the deviations from collision scaling are reduced. Hence we have to recalculate all hadron production at large p_{\perp} in Au–Au collisions and subsequently we have to introduce nuclear modifications to parton distributions and interactions of the scattering partons in the dense medium. These modifications have not yet been implemented so far.

The only thing we can present at the moment is a recalculation of large p_{\perp} π^0 production with DPMJET–III with full percolation and chain fusion and with the kinematical corrections to change the iteration procedure. In Fig.6 we present such DPMJET–III results and compare them to the RHIC data[37]. As expected, at larger p_{\perp} DPMJET–III produces a p_{\perp} distribution above the data.

5. Elliptic flow in DPMJET–III

The elliptic flow v_2 is defined as a Fourier coefficient of the single particle distribution [38,39]

$$v_2 = \langle \cos 2(\phi - \Phi_R) \rangle .$$

Φ_R is the orientation of the reaction plane and the angular brackets denote an average over many particles belonging to some phase–space region and over many collisions having approximately the same impact parameter. The elliptic flow v_2 is a sensitive probe of the dense matter produced in high–energy nucleus–nucleus collisions. Data from RHIC on v_2 were published by most RHIC Collaborations [40–43].

Quite a number of different methods have been proposed to extract the elliptic flow from data or from Monte Carlo models, it is not the purpose of this contribution to give an overview over these methods. Let us only mention two methods, which we use to analyze elliptic flow from DPMJET–III. One method uses in its simplest form two-particle cumulants [44]. The second method determines flow using Lee–Yang zeroes [45].

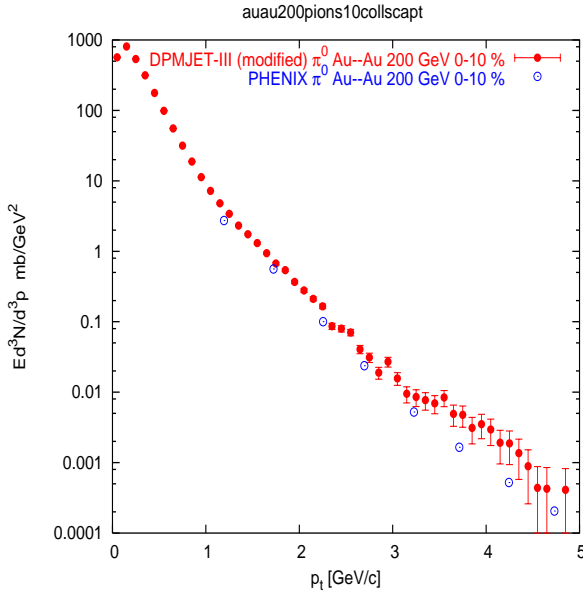


Figure 6. *Transverse momentum distribution of π^0 -mesons produced in central $\sqrt{s} = 200$ GeV Au–Au collisions. The results of the modified DPMJET-III are compared to experimental data from the PHENIX-Collaboration [37].*

We concentrate on Au–Au collisions at $\sqrt{s}_{NN} = 130$ GeV, for which experimental data for the integrated flow and for p_{\perp} dependent flow were presented in Ref. [43]. In a multichain model like DPMJET-III with non-interacting hadronic strings fragmenting into hadrons and for large secondary multiplicities, we expect of course a vanishing elliptic flow. But there are two effects in DPMJET-III which are expected to change this picture. The first effect is connected to the percolation of hadronic strings in DPMJET-III. An interaction of hadronic strings can be expected to also introduce a force between strings yielding some genuine elliptic flow. The second effect are jets and minijets in DPMJET-III. The number of large p_{\perp} jets and minijets at RHIC energies is not large, the jets produce significant azimuthal fluctuations, which leads to non-vanishing v_2 especially at large p_{\perp} .

In Table 1 we collect for two centralities (and the pseudorapidity acceptance of the experiment) some integrated flow values calculated with both

Table 1

Integrated flow: v_2 results obtained from DPMJET-III using two different methods (I: using two particle cumulants[44]; II: using Lee–Yang zeroes [45]; III: gives the spurious flow according to method II) to STAR data [43] from RHIC.

Centrality	particles	I	II	III	STAR
53–77 %	charged	0.0107	0.0140	0.047	0.07
53–77 %	π^{\pm}	0.0182	0.0135	0.051	
53–77 %	K^{\pm}	0.060	0.037	0.164	
0–5 %	charged	0.00685	0.00644	0.0129	0.02
0–5 %	π^{\pm}	0.00595	0.00693	0.0139	
0–5 %	K^{\pm}	0.0188	0.0215	0.0419	

methods mentioned above. In Fig.7 we compare the p_{\perp} dependent elliptic flow obtained from DPMJET-III using the two-particle cumulant method[44] for two different centralities to STAR data [43] from RHIC.

Let us discuss the results of the comparisons in Table 1 and Fig.7.

(i)The integrated flow values calculated from DPMJET-III with methods I and II agree reasonably well, however the spurious flow (column III of Tab. 1) calculated for method II indicates, that method II using Lee–Yang zeroes is not able to calculate the flow reliably. Also we find, that we are not able to calculate a significant p_{\perp} dependent flow using method II.

(ii)The integrated flow values in Table 1 calculated from DPMJET-III are significantly smaller than the experimental data from STAR, also we see in Fig.7 the p_{\perp} dependent flow at low p_{\perp} values (which dominate the particle production) is significantly smaller than the experimental data from STAR. We conclude: the flow introduced in the model by the percolation and fusion of chains is not enough to explain the data.

(iii)We find in Fig.7 that DPMJET-III at large p_{\perp} values shows larger flow than the data, this flow results from the jets and minijets as dis-

cussed above. This flow component in the experimental data is significantly smaller, we know that large p_{\perp} jets in the Au–Au data are strongly suppressed, the present version of DPMJET-III does not contain any mechanism for jet quenching.

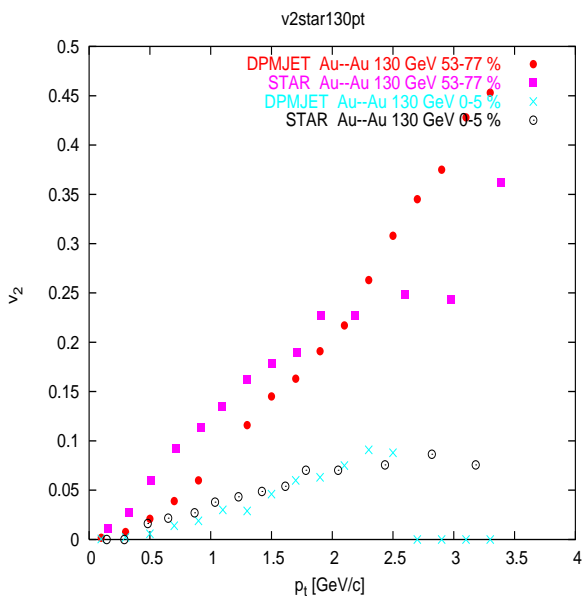


Figure 7. Elliptic flow v_2 as function of p_{\perp} in 130 GeV Au–Au collisions at RHIC. We compare for charged hadrons the DPMJET-III results for two centralities to experimental data from the STAR–Collaboration [43]

6. Summary

The data obtained at RHIC are extremely useful to improve hadron production models like DPMJET-III.

Of particular importance are data on hadron production in p–p collisions, d–Au collisions and peripheral Au–Au collisions, in all of these collisions (unlike central Au–Au collisions) we do not expect any change in the reaction mechanism, which could not be accommodated into the mechanisms as implemented in DPMJET-III.

Indeed, comparing DPMJET-III to RHIC data we find two important corrections to be applied to DPMJET-III, which otherwise do not completely change the independent chain fragmentation model: (i) Percolation and fusion of chains, the data from RHIC allow to determine the amount of percolation to be implemented into DPMJET-III. (ii) Collision scaling of large p_{\perp} hadron production in d–Au collisions: The data indicate that we have to change the iteration procedure (of the selection of all soft and hard chains in nuclear collisions) in such a way, that collision scaling is obtained.

REFERENCES

1. A. Capella, U. Sukhatme, C. I. Tan, and J. Trân Thanh Vân, Phys. Rep. **236**, 227 (1994).
2. R. Engel, Z. Phys. **C66**, 203 (1995).
3. R. Engel and J. Ranft, Phys. Rev. **D54**, 4244 (1996).
4. P. Aurenche *et al.*, Phys. Rev. **D45**, 92 (1992).
5. G. Veneziano, Nucl. Phys. **B74**, 365 (1974).
6. G. F. Chew and C. Rosenzweig, Phys. Rep. **41**, 263 (1978).
7. V. N. Gribov, Sov. Phys. JETP **26**, 414 (1968).
8. R. Engel, Ph.D. thesis, Universität Siegen, 1997.
9. F. W. Bopp, R. Engel and J. Ranft (unpublished).
10. A. Capella *et al.*, Phys. Rev. **D53**, 2309 (1996).
11. O. J. P. Eboli, E. M. Gregores and F. Halzen, Phys. Rev. **D58**, 114005 (1998).
12. B. Alper *et al.*, Nucl. Phys. **B87**, 19 (1975).
13. G. Arnison *et al.*, Phys. Lett. **B118**, 167 (1982).
14. F. Abe *et al.*, Phys. Rev. Lett. **61**, 1819 (1988).
15. T. Sjöstrand *et al.*, Comp. Phys. Commun. **135**, 238 (2001).
16. S. Roesler, R. Engel, and J. Ranft, Proceedings of ICRC 2001, Copernicus Ges. , (2001).
17. S. Roesler, R. Engel, and J. Ranft, hep-ph/0012252, Proc. of Monte Carlo 2000, Lisboa, Oct.2000, Springer, p.1033 , 1033 (2000).

18. J. Ranft, Phys. Rev. **D51**, 64 (1995).
19. J. Ranft, Siegen preprint SI-99-6, hep-ph/9911232 (unpublished).
20. S. Y. Shmakov, V. V. Uzhinskii, and A. M. Zadoroshny, Comp. Phys. Commun. **54**, 125 (1989).
21. J. Ranft, Phys. Rev. **D37**, 1842 (1988).
22. J. Ranft, R. Engel, and S. Roesler, hep-ph/0012112, Proc. of Monte Carlo 2000, Lisboa, Oct.2000, Springer, , 979 (2000).
23. J. Ranft, Siegen preprint Si-99-5, hep-ph/9911213 (unpublished).
24. J. Knapp *et al.*, Astropart. Phys. **19**, 77 (2003).
25. S.S.Adler et al, PHENIX Collaboration, hep-ex/0304038 (unpublished).
26. J. Dias de Deus and R. Ugoccioni, Phys. Lett. **B491**, 253 (2000).
27. J. Dias de Deus and R. Ugoccioni, Phys. Lett. **B494**, 53 (2000).
28. J. Dias de Deus, Y. M. Shabelski, and R. Ugoccioni, hep-ph/0108253 (unpublished).
29. M. Braun, F. del Moral, and C. Pajares, Phys. Rev. **C65**, 024907 (2002).
30. M. A. Braun, C. Pajares, and J. Ranft, Int. J. Mod. Phys. **A 14**, 2689 (1999).
31. M. Braun and C. Pajares, Eur. Phys. J. **C16**, 359 (2000).
32. I.G. Bearden et al, BRAHMS Collaboration, nucl-ex/0108016 (unpublished).
33. B. B.Back et al, PHOBOS Collaboration, nucl-ex/0201005 (unpublished).
34. K. Adcox et al, PHENIX Collaboration, nucl-ex/0012008 (unpublished).
35. B.B.Back et al, PHOBOS Colaboration , nucl-ex/0311009 (unpublished).
36. S.S.Adler et al, PHENIX Collaboration, Phys.Rev.Lett. **91**, 072303 (2003).
37. S.S.Adler et al, PHENIX Collaboration, Phys.Rev.Lett. **91**, 072301 (2003).
38. S. Voloshin and Y. Zhang, Z. Phys **C70**, 665 (1996).
39. J.-Y. Ollitrault, Phys. Rev. **D46**, 229 (1992).
40. K.Adcox et al, PHENIX Collaboration, Phys.Rev.Lett. **89**, 212301 (2002).
41. B.B.Back et al, PHOBOS Collaboration, Phys.Rev.Lett. **89**, 222301 (2002).
42. K.H.Ackermann et al, STAR Collaboration, Phys.Rev.Lett. **86**, 402 (2001).
43. C.Adler et al, STAR Collaboration, Phys.Rev. **C66**, 034904 (2002).
44. N.Borghini, P.M.Dinh and J.Y.Ollitrault, Phys.Rev. **C63**, 054906 (2001).
45. R.S.Bhalerao, N.Borghini and J.-Y.Ollitrault, nucl-th/0310016 (unpublished).